Original Article

Development and Validation of Cloud-based Heart Rate Variability Monitor

Sushma N. Bhat, Ghanshyam D. Jindal, Gajanan D. Nagare[1]

Department of Biomedical Engineering, MGM's College of Engineering and Technology, Navi Mumbai, [1]Department of Biomedical Engineering, VIT, Mumbai, Maharashtra, India

Abstract

Context: This article introduces a new cloud-based point-of-care system to monitor heart rate variability (HRV). **Aims:** Medical investigations carried out at dispensaries or hospitals impose substantial physiological and psychological stress (white coat effect), disrupting cardiovascular homeostasis, which can be taken care by point-of-care cloud computing system to facilitate secure patient monitoring. **Settings and Design:** The device employs MAX30102 sensor to collect peripheral pulse signal using photoplethysmography technique. The non-invasive design ensures patient compliance while delivering critical insights into Autonomic Nervous System activity. Preliminary validations indicate the system's potential to enhance clinical outcomes by supporting timely, data-driven therapeutic adjustments based on HRV metrics. **Subjects and Methods:** This article explores the system's development, functionality, and reliability. System designed is validated with peripheral pulse analyzer (PPA), a research product of electronics division, Bhabha Atomic Research Centre. **Statistical Analysis Used:** The output of developed HRV monitor (HRVM) is compared using Pearson's correlation and Mann–Whitney U-test with output of PPA. Peak positions and spectrum values are validated using Pearson's correlation, mean error, standard deviation (SD) of error, and range of error. HRV parameters such as total power, mean, peak amplitude, and power in very low frequency, low frequency, and high frequency bands are validated using Mann–Whitney U-test. **Results:** Pearson's correlation for spectrum values has been found to be more than 0.97 in all the subjects. Mean error, SD of error, and range of error are found to be in acceptable range. **Conclusions:** Statistical results validate the new HRVM system against PPA for use in cloud computing and point-of-care testing.

Keywords: Cloud computing, heart rate variability, photoplethysmography, stress monitoring

Received on: 31-08-2024 **Review completed on:** 25-09-2024 **Accepted on:** 07-10-2024 **Published on:** 18-12-2024

Introduction

Heart rate variability (HRV) refers to the fluctuations in the time intervals between consecutive systolic contractions, known as RR intervals. Unlike a metronome, a healthy heart exhibits complex and ever-changing rhythms, enabling the cardiovascular system to quickly adapt to sudden physical and psychological challenges to maintain homeostasis. Research have shown HRV parameters can be used as a promising prognosticator for many diseases such as diabetes, hypertension, and cardiac arrest.[1,2]

Wang *et al*.[3] initially established that time domain parameters of HRV are independent soothsayer for overall survival in brain metastasis patients and can be used for risk stratification in the future. Further extending the study in 2013, it was established that HRV is linked to survival and may serve as a new prognostic factor for patients with brain metastasis.[4] Highly significant difference has been observed in HRV parameters in variety of diseases such as hypertension, diabetes, coronary artery disease, cirrhosis of liver, rheumatoid arthritis, AIDS, lung cancer, and stomach cancer.[5] The European Task Force recommends at least 300 s of data for short-term analysis of HRV.[6] In cancer patient care, HRV can be used as biofeedback.[7] HRV can measure cancer-related fatigue,[8] predict the survival in patients with cancer,[9] objectively evaluate bone metastases pain[10] to mention few. Hence, it becomes a major medical decision support system.[11]

Impedance plethysmography instruments such as medical analyzer,[12] peripheral pulse analyzer (PPA)[13] help in

Access this article online	
Quick Response Code:	**Website:** www.jmp.org.in
	DOI: 10.4103/jmp.jmp_151_24

Address for correspondence: Mrs. Sushma N. Bhat, Research Scholar, Department of Biomedical Engineering, MGM's College of Engineering and Technology, Kamothe, Navi Mumbai, India. E-mail: bme.sushma@gmail.com

How to cite this article: Bhat SN, Jindal GD, Nagare GD. Development and validation of cloud-based heart rate variability monitor. J Med Phys 2024;49:654-60.

measurement and analysis of HRV parameters. Mandatory manual marking of first peak and subsequent manual intervention to make sure of accurate peak detection, apart from introducing human error, limit use of these instruments to laboratories or medical hospitals. To address these challenges, a new wearable device HRV monitor (HRVM) is developed using MAX30102 sensor. Sensor data are used in cloud computing to automatically compute, analyse, and report the HRV parameters. This development is described in this article.

Subjects and Methods

Hardware setup is shown in Figure 1. The Max 30102 sensor is utilized to capture pulse signals at a sampling frequency of 400 Hz. The configuration settings include a pulse width of 69 µs, an Analog to digital converter (ADC) range of 2048, and a sample average of 1. Few hardware adjustments optimize the sensor's performance, ensuring accurate pulse signal acquisition under the specified settings. Nano RP2040 microcontroller serves as an interface between the sensor and the desktop. The Nano RP2040 reads the data from the Max 30102 sensor, and then transmits these data to the desktop. This transmission typically occurs through a Universal serial bus (USB) connection, allowing the desktop to store the data for further processing in cloud server. The cloud server sends commands to the microcontroller to control data acquisition and storing processes.

The Nano RP2040 operates at a higher clock speed (up to 133 MHz) compared to many Arduino boards, enabling faster data acquisition and processing. It features a dual-core ARM

Table 1: Heart rate variability monitor peak detection validation with peripheral pulse analyzer

Subject	AP	CP	FP	FN	Percentage FN	Correlation	Mean absolute error (ms)	SD error (ms)	Range error (minimum–maximum) (ms)
F01	470	470	0	0		1	5.69	2.27	2.5–12.5
F02	472	470	0	2	0.42	1	5.39	2.22	2.5–12.5
F03	419	419	0	0	0.00	1	6.19	2.70	0–15
F04	449	449	0	0	0.00	1	5.48	2.81	0–12.5
M01	368	368	0	0	0.00	1	5.66	2.37	0–12.5
M02	450	450	0	0	0.00	1	4.88	2.12	2.5–12.5
F05	354	353	0	1	0.28	1	5.63	2.65	0–12.5
F06	368	368	0	0	0.00	1	4.86	1.79	0–12.5
F07	378	378	0	0	0.00	1	6.14	2.51	0–12.5
M03	437	437	0	0	0.00	1	5.27	1.88	2.5–12.5
M04	438	436	0	2	0.46	1	5.82	2.15	0–12.5
M05	370	370	0	0	0.00	1	5.01	1.97	2.5–12.5
M06	408	405	0	3	0.74	1	4.65	1.93	2.5–12.5
F08	393	393	0	0	0.00	1	5.06	1.98	2.5–12.5
F09	332	332	0	0	0.00	1	5.76	2.35	0–12.5
F10	396	396	0	0	0.00	1	5.48	2.25	0–12.5
F11	416	416	0	0	0.00	1	3.99	1.38	2.5–7.5
F12	412	412	0	0	0.00	1	5.73	2.31	0–12.5
F13	423	423	0	0	0.00	1	7.13	2.94	0–12.5
F14	371	371	0	0	0.00	1	5.90	2.40	2.5–12.5
F15	346	346	0	0	0.00	1	5.62	2.31	0–12.5
M07	331	329	0	2	0.60	1	6.05	2.47	0–12.5
M08	387	385	0	2	0.52	1	4.75	1.96	2.5–12.5
M09	336	334	0	2	0.60	1	4.76	1.87	2.5–12.5
M10	412	410	0	2	0.49	1	6.26	2.49	2.5–12.5
M11	339	339	0	0	0.00	1	6.79	2.55	2.5–12.5
M12	327	324	0	3	0.92	1	5.67	2.61	0–12.5
F16	342	342	0	0	0.00	1	5.19	2.14	2.5–12.5
F17	373	373	0	0	0.00	1	4.87	1.87	2.5–12.5
F18	444	444	0	0	0.00	1	4.99	1.89	2.5–12.5
F19	425	425	0	0	0.00	1	5.50	2.32	0–12.5
F20	454	450	0	4	0.88	1	4.98	2.24	2.5–12.5
F21	445	441	0	4	0.90	1	6.69	2.98	0–12.5
F22	414	412	0	2	0.48	1	5.86	2.43	0–12.5
F23	409	409	0	0	0.00	1	5.12	2.00	2.5–12.5
F24	489	489	0	0	0.00	1	4.46	2.57	0–12.5
F25	400	398	0	2	0.50	1	5.65	2.33	0–12.5

SD: Standard deviation, AP: Actual peak, CP: Confirmed detected peak, FP: False positive, FN: False negative

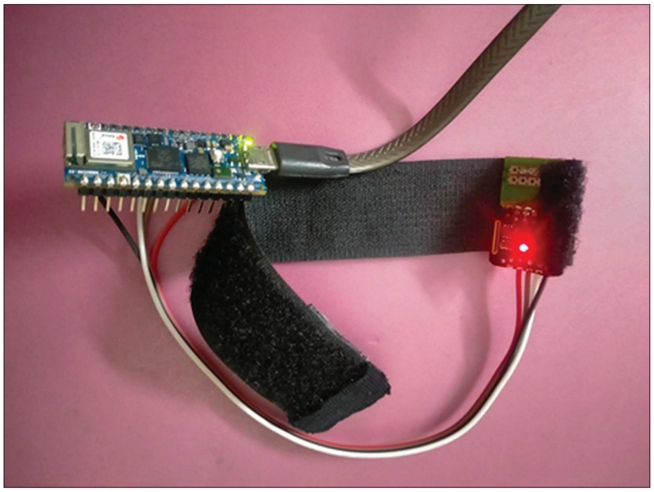

Figure 1: Sensor with Nano RP2040 in cloud-based HRVM system

Cortex-M0 + processor, providing better performance for multitasking and handling complex computations. The Nano RP2040 offers a wide range of communication interfaces, including I2C, Serial peripheral interface (SPI), and Universal asynchronous receiver transmitter (UART), which makes it more versatile for connecting additional peripherals alongside the Max 30102 sensor.

The NanoRP2040 microcontroller supports MicroPython. It can be in principle programmed to manage sensor data acquisition and processing. However, authors aim to develop a simple, robust device focused solely on data collection, with all signal processing conducted on a cloud server. This approach centralizes software updates, ensuring that any modifications to the processing algorithms occur in a single location. By decoupling signal acquisition from software updates, this system allows for independent upgrades of both hardware and

Table 2: Spectrum values of heart rate variability monitor compared with that of peripheral pulse analyzer

Participant code	Correlation of spectrum	*P*	Mean absolute error (ms^2)	SD error (ms^2)	Range error (ms^2)
F01	0.980	8.304E-91	−0.308	0.844	−3.244–1.921
F02	0.992	2.883E-114	−0.397	1.120	−4.723–6.171
F03	0.983	1.735E-94	−0.727	2.029	−10.487–3.195
F04	0.996	1.709E-131	−0.312	2.716	−11.150–15.533
M01	0.974	6.910E-83	0.164	4.412	−3.685–45.086
M02	0.981	4.058E-92	−0.006	0.572	−2.016–2.560
F05	0.995	1.666E-127	−3.097	16.103	−146.633–0.333
F06	0.993	1.515E-119	−0.110	2.540	−13.272–9.335
F07	0.995	2.933E-126	−1.108	5.702	−54.503–6.920
M03	0.990	7.151E-109	−0.581	1.600	−6.368–4.310
M04	0.993	3.705E-118	−0.329	1.205	−5.295–2.786
M05	0.998	9.089E-159	−0.275	1.794	−7.378–12.699
M06	0.993	1.334E-120	−0.485	1.708	−9.494–8.211
F08	0.999	1.530E-162	−0.127	0.882	−5.077–3.604
F09	0.998	4.923E-155	−0.351	1.318	−10.060–2.653
F10	0.996	1.944E-133	−0.033	0.954	−1.907–3.563
F11	0.995	2.619E-128	−0.187	0.698	−4.505–3.933
F12	0.994	3.363E-124	−0.881	2.232	−8.085–9.097
F13	0.988	5.808E-104	−0.957	4.855	−27.818–15.667
F14	0.998	4.908E-153	0.007	1.720	−4.160–12.583
F15	0.986	1.050E-99	0.039	2.304	−4.051–17.059
M07	0.992	9.124E-116	−0.659	2.649	−12.038–16.993
M08	0.993	1.031E-119	−0.993	2.995	−19.374–5.711
M09	0.994	3.489E-121	−0.675	2.227	−11.935–6.226
M10	0.987	5.955E-102	−0.394	1.330	−5.956–3.004
M11	0.994	3.523E-121	−0.428	1.274	−4.271–8.770
M12	0.988	1.371E-103	−1.110	3.136	−11.906–15.076
F16	0.994	8.309E-121	−0.822	3.416	−20.530–16.641
F17	0.995	1.663E-130	−0.409	0.895	−4.815–3.149
F18	0.990	7.202E-108	−0.564	2.174	−19.030–3.725
F19	0.998	4.124E-156	−0.150	2.715	−12.637–13.313
F20	0.990	2.271E-108	−0.282	1.339	−7.464–7.147
F21	0.987	6.738E-102	−0.367	1.111	−5.761–2.391
F22	0.991	3.285E-113	−0.612	1.219	−7.025–1.954
F23	0.994	2.851E-121	−0.124	0.618	−2.858–2.856
F24	0.988	1.509E-104	−0.128	0.914	−6.634–1.631
F25	0.996	8.531E-137	−0.273	0.890	−4.038–4.140

SD: Standard deviation

software components. Moreover, processing signals on the cloud provides the advantage of using a standardized algorithm to analyze pulse signals from any photoplethysmography device with a sampling frequency of 400 Hz. A prototype desktop application was developed and tested as a precursor to a cloud-based solution. The application was implemented in python, chosen for its compatibility with cloud deployment environments. The program is designed to read data stored in a text file and perform necessary processing tasks. This preliminary development phase allows for seamless transition to a cloud infrastructure, where the python-based application can be deployed and scaled efficiently, leveraging the cloud's computational resources for data processing.

The sensor data, being a photoplethysmographic signal, initially presented as a mirror image of the actual physiological signal. This inversion was corrected, and an offset adjustment was performed before applying a low-pass filter (2nd order, 15 Hz Cutoff).[14] The rate of change of blood volume (blood flow) in the respective area is determined using the first time derivative of this filtered signal. Figure 2 outlines the steps involved in signal acquisition and peak detection.

Ventricular systole lasts approximately 0.3 s. corresponding to 20 samples for each systolic phase. Based on this, a window of 120 samples is formed, and its variance (V_i) and maximum value (C_i) are calculated. The window is then shifted by 10 samples, and the process is repeated. This ensures that within one cardiac cycle, at least one window will align closely with the ventricular systole. The variance of this window is typically the highest (V^m_i) compared to the neighboring windows, ensuring the signal's absolute value is included in the study. During a peak, the maximum value of the window tends to remain constant for around 12 consecutive windows. The sample number (S_n) corresponding to these repetitive maxima is saved. This is shown in Figure 3. To confirm whether the detected peak is a true systolic peak, confirmation of the same is required, as some peaks might be caused by noise or motion artifacts and could result in false positives. Similarly, a real peak may go undetected, leading to a false negative. To reduce these errors, the detected peaks pass through a peak qualifying algorithm. Flowchart of the same is shown in Figure 4. Using the sample numbers (S_n) where the maxima occur, a CC-interval array is generated, representing the time between consecutive systolic peaks, which closely matches the RR-interval of the electrocardiogram. For qualifying the peak, each CC-interval must fall within 0.7–1.3 times the average of the previous five CC-intervals ($\overline{CC}$). This helps to reject false positives in nonarrhythmic subjects. If a CC-interval exceeds 1.3 times the average, it may indicate a missed beat or a false negative peak which is taken care by interpolation in subsequent steps. If there is a gap exceeding five CC-intervals in peak detection, it is flagged as a data error. Updating the CC-interval beyond this point is not recommended.[6] The output of HRVM is validated against PPA (an R and D product of Electronics Division, Bhabha Atomic Research Centre).[15] It uses impedance plethysmography to measure electrical impedance and its time derivative at three consecutive segments in the left arm nearing to wrist. These signals are processed and analyzed using a desktop application. This software analyses the data with the help of time domain parameters, frequency domain parameters, and Poincaré plot.[16] This instrument is robust and has been extensively used by medical fraternity[17] and for research purpose. In PPA, peak detection plays a crucial role. After visual inspection, first peak is marked manually. Subsequent peaks are marked by the software. Thus, marked peaks are reviewed for false positives and false negatives. This is followed by manual editing of detected peak positions

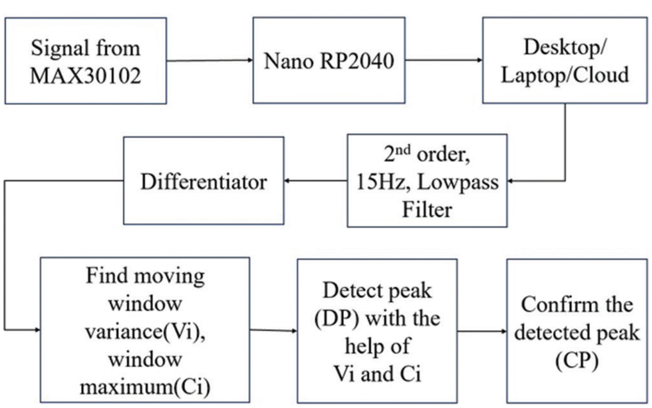

Figure 2: Simplified block diagram of heart rate variability monitor and flow of peak detection

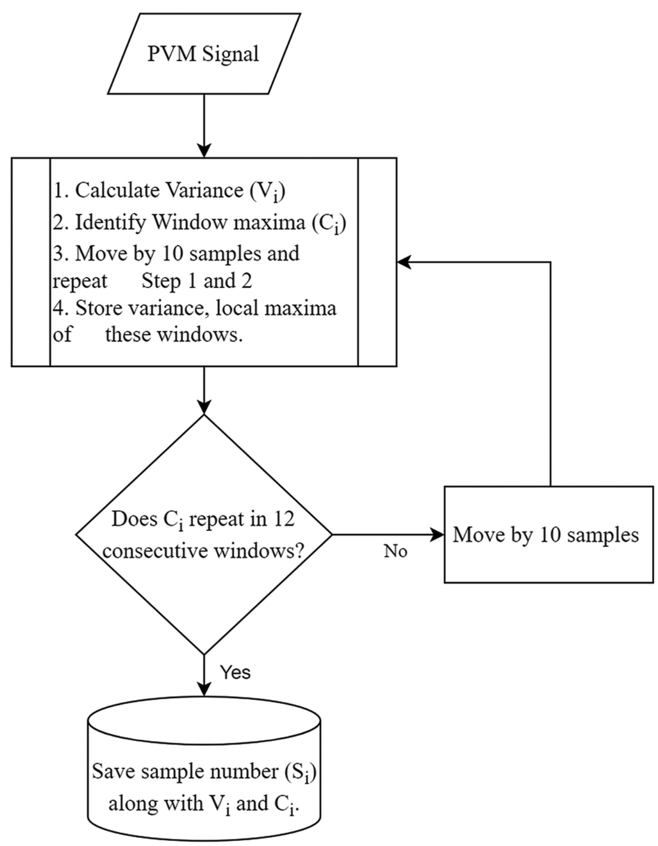

Figure 3: Peak detection algorithm

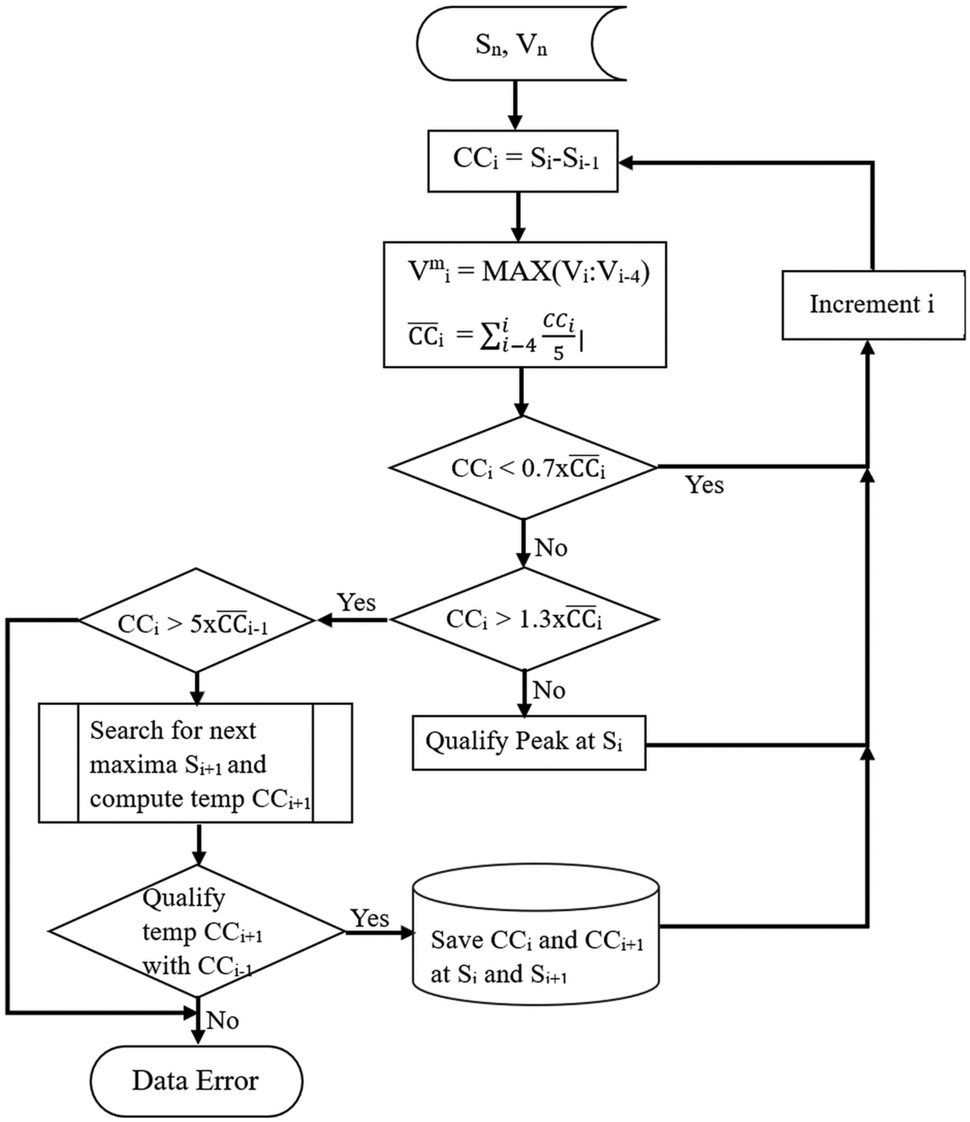

Figure 4: Peak qualifying algorithm

if necessary. Currently, this manual intervention makes the procedure offline as well as limits the usage only to trained professionals. Thus, introducing latency period for processing and result generation.

For the current study, peripheral pulse data are collected from 37 healthy participants (12 males, 25 females in age bracket of 30–55 years) using PPA and HRVM simultaneously. Informed written consent is signed by each individual. This data collection protocol is reviewed and approved by institutional ethics committee. Performance of the algorithm for peak detection is analyzed using Pearson correlation mean absolute error, standard deviation (SD) of error, and range error.

From the identified peaks, the RR intervals are extracted. These RR values are interpolated to create a uniformly spaced time series, enabling the application of Fast fourier transform (FFT) to derive frequency domain parameters. Obtained spectrum is compared in the manner similar to that for RR intervals. Frequency domain parameters such as total power, mean, peak amplitude, and power of in very low frequency (VLF), LF and high frequency (HF) bands are calculated from PPA and HRVM spectra and validated with the help of Mann–Whitney U-test. The next step would be to deploy the application on cloud server.

Deploying a python application on Amazon Web Services (AWS) involves several steps, ensuring a scalable and reliable environment for the application. After logging into the AWS Management Console, an EC2 instance is created. This serves as virtual server. Ubuntu is chosen as Amazon Machine Image and instance type, security groups, and key pair for Secure socket shell (SSH) access are configured.

Once the instance is launched, it is connected through SSH, and python environment is set up. This typically involves installing necessary packages, such as python and git, and creating a virtual environment. Application's code repository is cloned. Required dependencies are installed before running the application.

To ensure the application is accessible over the internet, an Elastic IP with EC2 instance is associated. This static IP address ensures the application remains accessible even if the instance is stopped and restarted. Figure 5 shows the Ubuntu system up and running ready to execute HRVM application.

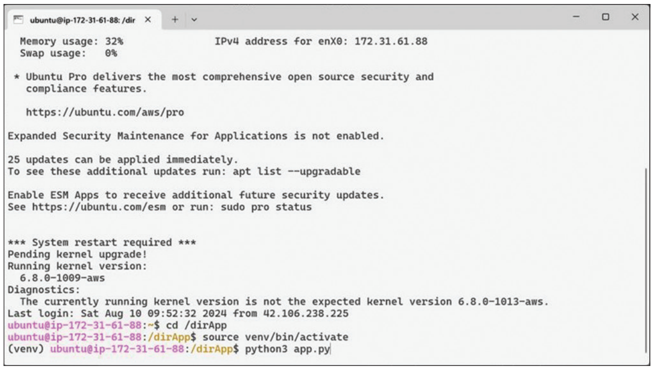

Figure 5: Command prompt showing the appliction ready for execution on ubuntu virtual environment

Results and Discussions

Table 1 gives the performance of automatic peak detection in HRVM against conventional interactive peak detection in PPA. As observed, there is no false positive. Few false negatives observed can be ignored as the entire series undergo interpolation, which is vulnerable only to false positives. Maximum error is observed to be 15 ms on an average RR-interval value of 750 ms (2%) which is within the acceptable limit of 5%.

Table 2 gives similar analysis of power spectral density derived from HRVM against that from PPA. It is observed that the correlation coefficient is more than 0.974 with probability of being different <6.910E-83 suggesting acceptable performance of python-based approach. It is difficult to comment on mean, SD, and range of error as magnitude of spectral component has wide variation (from 0.0086 to 23.7497).

Table 3 gives the comparison of HRV parameters derived from HRVM and PPA by Mann–Whitney U-test. It is observed that

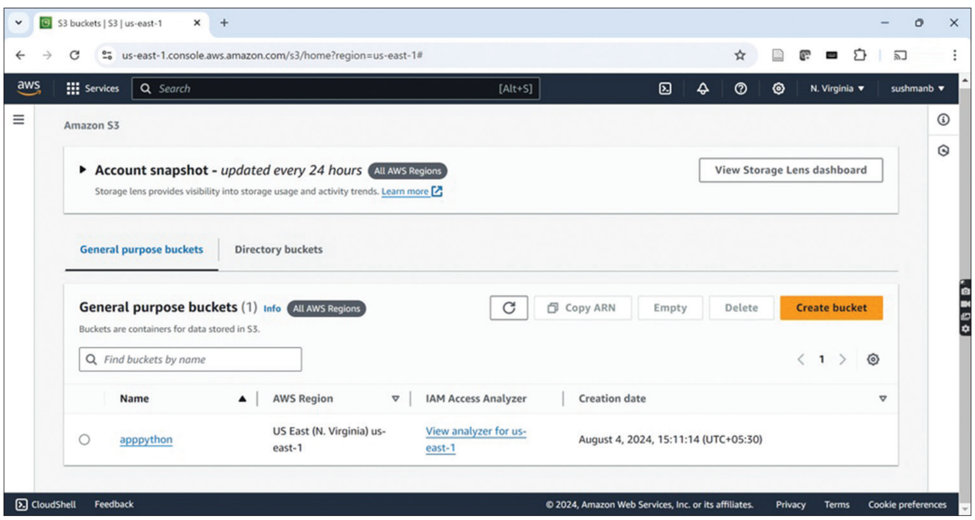

Figure 6: Screen grab of the application in AWS cloud server. AWS: Amazon Web Services

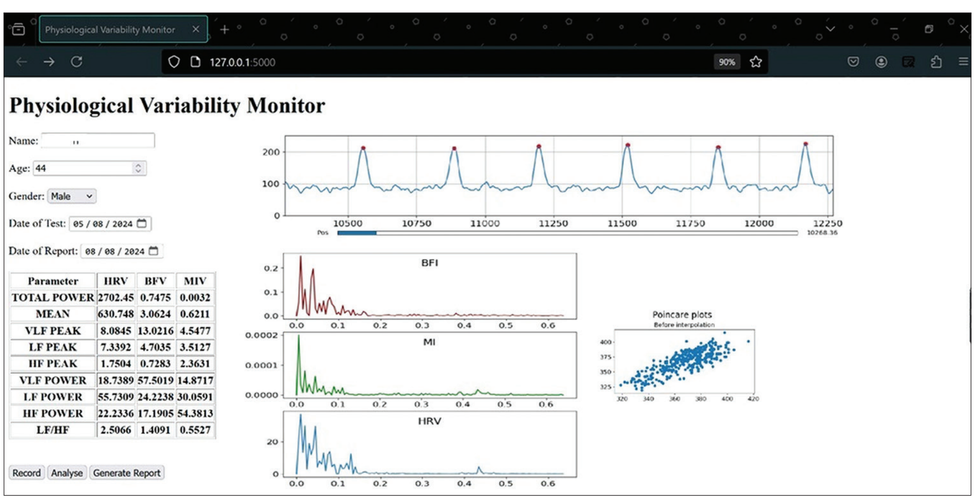

Figure 7: Screen grab of the application showing parameter values and variability plots

Table 3: Mann–Whitney *U*-test results on heart rate variability parameters

Parameter	*Z*	*P*
Total power	0.492	0.312
Mean	−0.178	0.452
VLF amp	−1.097	0.117
LF amp	−1.108	0.117
HF amp	0.816	0.209
VLF power	0.222	0.413
LF power	−1.141	0.125
HF power	2.849	0.002

LF: Low frequency, HF: High frequency, VLF: Very LF

P value is more than 0.05 for all parameters except the HF power. It therefore validates values of total power, mean, VLF amp, LF amp, HF amp, VLF power, and LF power, however, HF power value is not compatible with that from PPA.

Validated PVM application is deployed on AWS Cloud. Screen grab of the cloud server is shown in Figure 6. Figure 7 shows the web server response with the application.

Financial support and sponsorship

Nil.

Conflicts of interest

There are no conflicts of interest.

References

1. Sawant M, Jindal GD, Agarwal S, Deshpande AK. Original article study of heart rate variability in control and hypertensive subjects. Indian Journal of Physiology and Pharmacology 2019;63:113-121.
2. Rajendra Acharya U, Paul Joseph K, Kannathal N, Lim CM, Suri JS. Heart rate variability: A review. Med Biol Eng Comput 2006;44:1031-51.
3. Wang YM, Wu HT, Huang EY, Wang CJ, Hseu SS, Kou YR. A novel prognostic factor in patients with brain metastasis: Heart rate variability. Int J Radiat Oncol Biol Phys 2015;93:E472-3.
4. Wang YM, Wu HT, Huang EY, Kou YR, Hseu SS. Heart rate variability is associated with survival in patients with brain metastasis: A preliminary report. Biomed Res Int 2013;2013:503421.
5. Jindal G, Sawant MS, Jain RK, Bhat SN, Alva J, Rao S, *et al*. Study of variability in heart rate, peripheral blood flow and pulse wave morphology index in health and disease. MGM J Med Sci 2018;5:101-8.
6. Malik M, Thomas Bigger J, John Camm A, Kleiger RE, Malliani A, Moss AJ *et al*. Heart rate variability: Standards of measurement, physiological interpretation, and clinical use, European Heart Journal, 1996;17:354-381. Available from: https://doi.org/10.1093/oxfordjournals.eurheartj.a014868.
7. Spada GE, Masiero M, Pizzoli SF, Pravettoni G. Heart rate variability biofeedback in cancer patients: A scoping review. Behav Sci (Basel) 2022;12:389.
8. Shih CH, Chou PC, Chen JH, Chou TL, Lai JH, Lu CY *et al*. Cancer-related fatigue classification based on heart rate variability signals from wearables. Front Med (Lausanne). 2023;10:1103979. doi: 10.3389/fmed.2023.1103979.
9. Zhou X, Ma Z, Zhang L, Zhou S, Wang J, Wang B, *et al.* Heart rate variability in the prediction of survival in patients with cancer: A systematic review and meta-analysis. J Psychosom Res 2016;89:20-5.
10. Murofushi K, Murofushi W, Komazawa M, Ohnishi K, Shimizuguchi T, Ito K, *et al*. Preliminary study on establishing a heart rate variability – Based method for objectively evaluating bone metastasis pain. Int J Radiat Oncol Biol Phys 2022;114:e447.
11. Faust O, Hong W, Loh HW, Xu S, Tan RS, Chakraborty S, *et al.* Heart rate variability for medical decision support systems: A review. Comput Biol Med 2022;145:105407.
12. Ananthakrishnan TS, Jindal GD, Sinha V, Jain RK, Kataria SK, Deshpande AK. Clinical validation of software for a versatile variability analyzer: Assessment of autonomic function. J Med Phys 2007;32:97-102.
13. Warrier JS, Deshpande AK, Athavale PP, Bagal UR, Rajput M. 'Peripheral Pulse Morphology for Early Detection of Coronary Artery Disease', MGM Journal of Medical Sciences, 2016;1:112–116. doi: 10.5005/jp-journals-10036-1019.
14. Shankar TM, Webster JG. Design of an automatically balancing electrical impedance plethysmograph. J Clin Eng 1984;9:129.
15. Jindal GD, Jain RK, Sinha V, Mandlik SA, Bhagyashree S, Pooja T, *et al*. Early detection of coronary heart disease using peripheral pulse analyzer, BARC Newsletter, 2012;326:15-21.
16. Bhat SN, Jindal GD, Xavier M, Wagh RD, Garje KS, Nagare GD. Poincare Plot: A Simple and Powerful Expression of Physiological Variability. MGM J Med Sci. Available from: https://web.archive.org/web/20220709165913id_/https://www.mgmjms.com/article.asp?issn=2347-7946;year=2021;volume=8;issue=4;spage=435;epage=441;aulast=Bhat. [Last accessed on 2024 May 02].
17. Jain RK, Goyal S, Bhat SN, Rao S, Sakthidharan V, Kumar P, *et al.* Development of software for automatic analysis of intervention in the field of homeopathy. J Altern Complement Med 2018;24:422-30.